

1104
495

9 MAR 1948

NATIONAL ADVISORY COMMITTEE FOR AERONAUTICS

TECHNICAL NOTE

No. 1541

THE EFFECT OF WING BENDING DEFLECTION ON THE
ROLLING MOMENT DUE TO SIDESLIP

By Powell M. Lovell, Jr.

Langley Memorial Aeronautical Laboratory
Langley Field, Va.



Washington

February 1948

LIBRARY COPY

APR 3 1993

LANGLEY RESEARCH CENTER
LIBRARY NASA
HAMPTON, VIRGINIA

NACA LIBRARY
LANGLEY MEMORIAL AERONAUTICAL
LABORATORY
Langley Field, Va.



3 1176 01434 0591

NATIONAL ADVISORY COMMITTEE FOR AERONAUTICS

TECHNICAL NOTE NO. 1541

THE EFFECT OF WING BENDING DEFLECTION ON THE
ROLLING MOMENT DUE TO SIDESLIP

By Powell M. Lovell, Jr.

SUMMARY

A method is presented for calculating the effect of wing flexibility on the rolling moment due to sideslip for wings of various aspect ratios and taper ratios when different shapes of the bending-deflection curve are assumed. The shape of the deflection curve is shown to be unimportant, the main factor being the amount of wing-tip deflection. An accurate and an approximate method for calculating the tip deflection are given. The effect of wing flexibility on the rolling moment due to sideslip seems to be large enough to be of appreciable importance in the design of large low-load-factor airplanes.

INTRODUCTION

The tendency toward thinner wings on both fighter and bomber airplanes and the tendency toward high aspect ratios on bomber and transport airplanes makes the effects of wing flexibility assume greater importance than heretofore. In some phases of aeronautical engineering wing flexibility must be taken into account in complying with design rules, but the effect of wing bending on the stability parameter for the rolling moment due to sideslip has not heretofore been investigated in detail.

Results are presented of an analysis made to determine the magnitude of the effect of wing bending on the rolling moment due to sideslip and a method is given by which the effective dihedral may be modified at the design stage to take into account the effect of wing bending. The results are applicable to either straight wings or slightly sweptback wings. Although the method is based on an application of the lifting-line theory to straight wings and hence might seem limited to subsonic speeds, it may be used to give approximate values at higher speeds.

SYMBOLS

$C_{l\beta}$	rate of change of rolling-moment coefficient C_l with side-slip angle β
Γ	dihedral angle, radians
b	wing span, inches
y	spanwise distance, inches
n	load factor
n_l	limit load factor
m	exponent designating shape of wing deflection curve
S	wing area, square inches
A	wing aspect ratio (b^2/S)
λ	taper ratio; that is, ratio of fictitious tip chord, obtained by extending wing leading and trailing edges to tip, to root chord
F	yield strength of metal of spar flange, pounds per square inch
σ	stress, pounds per square inch
E	modulus of elasticity, pounds per square inch
c	distance to outer fiber, inches
k	portion of semispan $\left(\frac{y}{b/2}\right)$
t	wing thickness, inches
z	deflection of wing, inches
M	wing bending moment, inch-pounds
I	moment of inertia, inches ⁴
Subscripts	
r	root
t	tip

DISCUSSION

Determination of Increment in Rolling-Moment Coefficient

Due to Sideslip with Wing Bending

In reference 1 influence lines showing the contribution of unit lengths of dihedral portions along the span to the rolling-moment derivative due to sideslip of a rigid wing were given. These results are given in figure 1 of the present paper. The wings considered had aspect ratios of 6, 10, and 16 and taper ratios of 0.25, 0.50, and 1.0.

The curves of figure 1 are readily adaptable to the determination of either the effective dihedral change due to a specified shape of bending curve or to the determination of the increment in rolling-moment coefficient due to sideslip.

If it is assumed that the deflection curve of the wing is given by

$$z = z_t \left(\frac{y}{b/2} \right)^m \quad (1)$$

then the dihedral angle Γ at any position along the span is

$$\Gamma = \frac{dz}{dy} = m \left(\frac{z_t}{b/2} \right) \left(\frac{y}{b/2} \right)^{m-1} \quad (2)$$

From the curves shown in figure 1 the elemental contribution of a unit dihedral angle extending a distance dk along the span to the increment in the rolling-moment derivative is

$$\Delta(\Delta C_{l_\beta}) = \frac{d \left(\frac{\Delta C_{l_\beta}}{\Gamma} \right)}{dk} \Gamma dk \quad (3)$$

Substituting the value of Γ from equation (2) into equation (3) and integrating across the span gives the following equation for the increment in the rolling-moment derivative due to wing deflection:

$$\Delta C_{l_\beta} = m \left(\frac{z_t}{b/2} \right) \int_0^1 \frac{d \left(\frac{C_{l_\beta}}{\Gamma} \right)}{dk} (k)^{m-1} dk \quad (4)$$

Equation (4) was integrated graphically by using the results obtained from figure 1, for values of the exponent m corresponding to various shapes of the wing bending curve. The results of these integrations are

shown in figure 2 where the ratio $\frac{\Delta C_{l\beta}}{z_t/b/2}$ is plotted against aspect

ratio A with taper ratio λ and bending-curve exponent m as parameters.

Values from figure 2 have been used to form a ratio of the coefficients obtained for various values of the exponent m to those for the case where $m = 1$. These ratios, which indicate how the particular shape of the bending-curve affects the increment in rolling-moment derivative due to sideslip, are shown in figure 3. It can be seen from

figure 3 that in the range of m from 2 to 6 the ratio $\frac{(C_{l\beta})_m}{(C_{l\beta})_{m=1}}$ changes very little. The curve of figure 3 is for an aspect ratio of 6 and a taper ratio of 0.50.

The values of the ratio $\frac{(C_{l\beta})_m}{(C_{l\beta})_{m=1}}$ have been tabulated in table 1

for all combinations of aspect ratio and taper ratio considered. Thus it appears that the particular exponent of the wing deflection curve is relatively unimportant as compared with the wing-tip deflection.

Figure 4 is a plot of $\frac{C_{l\beta}}{r}$ against A for a rigid wing ($m = 1$)

with taper ratio as a parameter. The curves of figure 4 were obtained by cross-plotting the points of figure 1 at the tip against aspect ratio and interpolating curves for taper ratios of 0.375 and 0.75. Figure 4 and table 1 when used together comprise the best method for calculating the increment in rolling moment due to wing flexibility.

Wing Deflection

Since the actual tip deflection is important in the determination of the increment in $C_{l\beta}$ due to wing flexibility, two methods of calculating this quantity are given which may be used in lieu of actual test data.

The more accurate method for obtaining the tip deflection requires a knowledge of the moments of inertia of the strength members of the wing at various spanwise stations, of the bending moment at these stations, and of the modulus of elasticity of the material. The method is based on the formula

$$z = \int \int \frac{M}{EI} \quad (5)$$

Figures 5, 6, and 7 show the $\frac{M}{EI}$ -curves at the limit load factor for typical fighter-type and bomber-type airplanes (data obtained from

manufacturers' reports). An approximation of these curves may be obtained by using fewer spanwise stations. The calculations that will be required if little or no information concerning moments of inertia of structural members is available will be considerably decreased thereby. A knowledge of the locations of heavy weight items and cut-outs in the wing structure is of value in choosing the best stations at which to perform calculations, because at these locations the moment of inertia may change rapidly (fig. 6). The percentage of error incurred by using the smaller number of stations (dashed curves of figs. 5 to 7) instead of the larger number was greatest for the fighter-type airplane of figure 6 which gave a 4.3 percent larger tip deflection at the limit load factor.

An approximate method for calculating tip deflections has been developed which may be used if information concerning the moments of inertia of structural members is not available. The following equation applying to a cantilever beam is the basis for this method:

$$\frac{d^2 z}{dy^2} = - \frac{\sigma}{Eg} \quad (6)$$

In this equation the fiber stress σ varies along the span according to the spanwise loading distribution. From practical considerations the fiber stress will always decrease toward the wing tip; however, in order to obtain a simple equation for estimating the tip deflection, it is convenient to assume a uniform effective value of σ over the span. This effective value of σ for the limit loading conditions is obtained by applying a reduction factor to the yield strength F of the spar flange material. From calculations involving five airplanes in which the factor ranged from 0.455 to 0.493, an average value of 0.47 was obtained for this reduction factor. The necessity for a reduction factor may be ascribed to causes such as the following:

- (1) The working stress over flanges and stringers is considerably below the yield strength of the flanges
- (2) No allowance is made for shear lag and torsion bending stresses
- (3) A nonuniformity of spanwise distribution of working stress exists

The factor 0.47 should be considered as only directly applicable to stressed-skin, semimonocoque construction with spanwise stiffeners of conventional construction.

If it is assumed that $\frac{t_t}{t_r}$ is the taper ratio, which makes the

distance c vary uniformly along the span, equation (6) may be written

$$\frac{d^2 z}{dy^2} = -0.47 \frac{n}{n_1} \frac{F}{E} \frac{b}{\left(\frac{b}{2} - y\right) t_r + y t_t} \quad (7)$$

By making use of the conditions that $z = \frac{dz}{dy} = 0$ when $y = 0$ and by introducing the notation that $\frac{y}{b/2} = k$, the equation for the tip deflection becomes, after a double integration,

$$\frac{z_t}{\frac{0.47 n F b^2}{n_1 E (t_r - t_t)}} = \frac{1}{2} \int_0^1 \log_e \frac{1}{1 - k \left(1 - \frac{t_t}{t_r}\right)} dk \quad (8)$$

Figure 8 shows the variation of the right side of equation (8) with the thickness ratio (taper ratio) $\frac{t_t}{t_r}$. For the case in which $\frac{t_t}{t_r}$ equals 1.0, equation (8) becomes indeterminate and the tip deflection may be obtained from the equation

$$z_t = - \frac{0.47 n F b^2}{4 n_1 E t_r} \quad (9)$$

The tip deflections determined from both methods have been compared with those obtained from Army Air Forces and manufacturers' reports of static tests of typical fighter-type and bomber-type airplanes. The results obtained by using the $\frac{M}{EI}$ -formula are within 7 percent of the measured values, whereas those obtained by use of the approximate formula are within 15 percent of the measured values for these airplanes.

Illustrative Example

In order to illustrate the use of table 1 and figure 4 in determining the effect of wing flexibility on the rolling-moment derivative due to sideslip, an example is worked for a hypothetical fighter airplane with characteristics as follows:

Wing span, inches	444
Wing aspect ratio	6
Wing taper ratio	0.50
Limit load factor	8
Dihedral angle, radians	0.0873
Modulus of elasticity for dural, pounds per square inch	10,500,000

From figure 6 the tip deflection at the limit load factor equals 9.12 inches. For level flight at 1g the tip deflection equals 1.14 inches. From figure 1 the value of C_{l_β} for the rigid wing with a dihedral angle of 0.0873 radians is

$$C_{l_\beta} = \frac{C_{l_\beta}}{\Gamma} \Gamma = 0.745 \times 0.0873 = 0.0650$$

The increment in C_{l_β} , ΔC_{l_β} , due to the wing bending at 1g for $m = 2$ is found to be, by using the value 0.745 from figure 4 and the value 1.21 from table 1,

$$\Delta C_{l_\beta} = \frac{\Delta C_{l_\beta}}{\Gamma} \frac{z_t}{b/2} = 0.745 \times 1.21 \times \frac{1.14}{222} = 0.0047$$

From equation (2) it can be determined that for a rigid wing ($m = 1$),

$$\frac{z_t}{b/2} = \Gamma$$

The recommendation for using parabolic ($m = 2$) bending is justified since parabolic bending agrees well with typical static test results.

It can be seen that at 1g the increment in C_{l_β} is relatively small compared with the rigid-wing value but that at higher load factors the increment becomes more important. In order to indicate the importance of wing flexibility on C_{l_β} for other types of airplanes, computations were carried out for a hypothetical bomber airplane with $A = 10$, $\lambda = 0.50$, and $\Gamma = 40$. The results are given in table 2 along with results for the fighter airplane. It will be noted that even at 1g the effect of wing flexibility on the bomber airplane is to increase the value of C_{l_β} by one-third, and at the limit load factor the value is almost doubled. Thus for large airplanes operating at relatively low load factors, the change in the derivative C_{l_β} is large enough to influence the control effectiveness in accelerated turns and should be taken into account at the design stage.

CONCLUSIONS

A relatively simple method has been devised by which the effect of wing elasticity on the effective dihedral and on the derivative in rolling-moment coefficient due to sideslip may readily be determined for wings of various aspect ratios and taper ratios when different shapes of the

bending-deflection curve are assumed. The shape of the bending-deflection curve is relatively unimportant in determining the effects of wing flexibility on the rolling moment due to sideslip, the main factor being the amount of wing-tip deflection. The effect of wing flexibility on the rolling-moment due to sideslip seems to be large enough to be of appreciable importance in the design of large low-load-factor airplanes.

Langley Memorial Aeronautical Laboratory
National Advisory Committee for Aeronautics
Langley Field, Va., November 3, 1947

REFERENCE

1. Pearson, Henry A., and Jones, Robert T.: Theoretical Stability and Control Characteristics of Wings with Various Amounts of Taper and Twist. NACA Rep. No. 635, 1938.

TABLE 1
 VARIATION OF ROLLING-MOMENT DERIVATIVE RATIO WITH
 ASPECT RATIOS AND TAPER RATIOS

Aspect ratio	Taper ratio	$\frac{(C_{l\beta})_{m=2}}{(C_{l\beta})_{m=1}}$	$\frac{(C_{l\beta})_{m=3}}{(C_{l\beta})_{m=1}}$
6	1.00	1.22	1.29
	.50	1.21	1.24
	.25	1.16	1.15
10	1.00	1.22	1.29
	.50	1.21	1.26
	.25	1.18	1.22
16	1.00	1.30	1.33
	.50	1.24	1.29
	.25	1.20	1.21



TABLE 2

INCREMENT IN ROLLING-MOMENT COEFFICIENT DUE TO SIDESLIP
 FOR TYPICAL CONTEMPORARY FIGHTER-TYPE AND BOMBER-TYPE AIRPLANES
 WITH VARIOUS LOAD FACTORS

	Fighter	Bomber
Aspect ratio	6	10
Taper ratio	0.50	0.50
Dihedral angle, deg	5	4
Limit load factor	8	2.67
$C_{l\beta}$ for rigid wing	0.0650	0.0613
Increment $C_{l\beta}$ for load factor of 1	0.0047	0.0212
Increment $C_{l\beta}$ for one-half limit load factor	0.0188	0.0283
Increment $C_{l\beta}$ for limit load factor	0.0376	0.0566



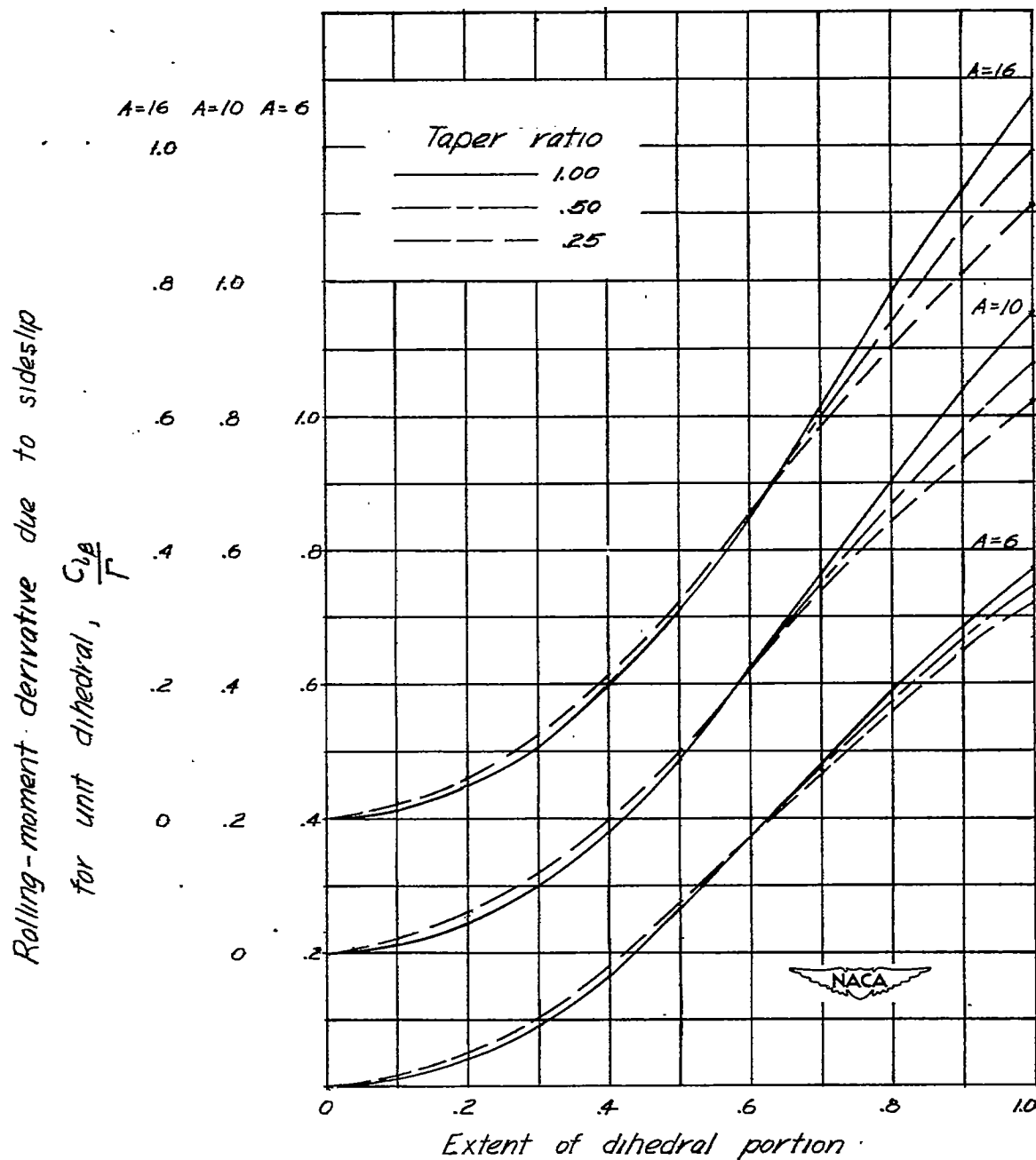


Figure 1.—Rolling-moment derivative due to sideslip
plotted against extent of dihedral portion.
(From fig. 16 of reference 1.)

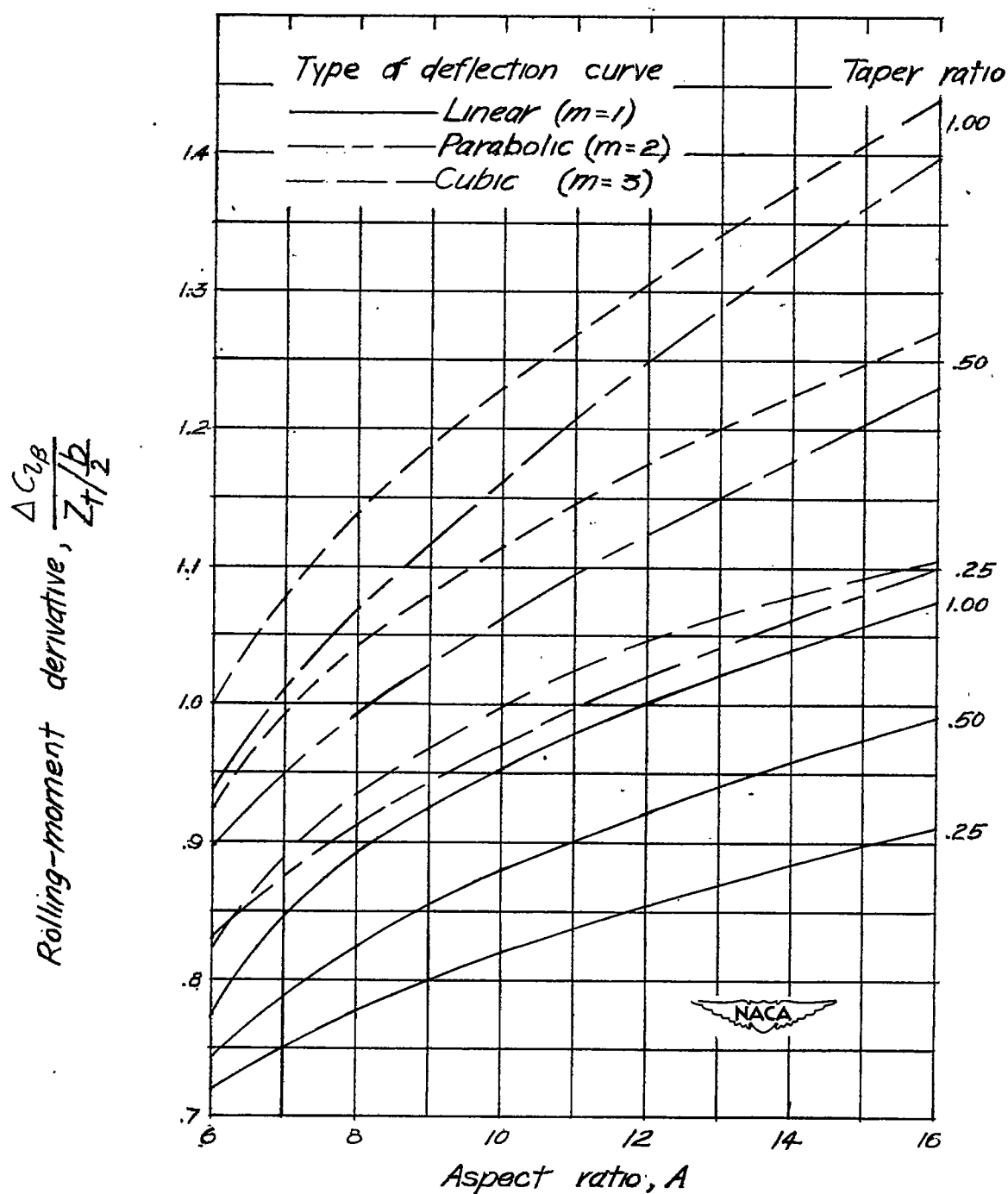


Figure 2.— Variation of increment in rolling-moment derivative with aspect ratio and taper ratio for several types of deflection curves.

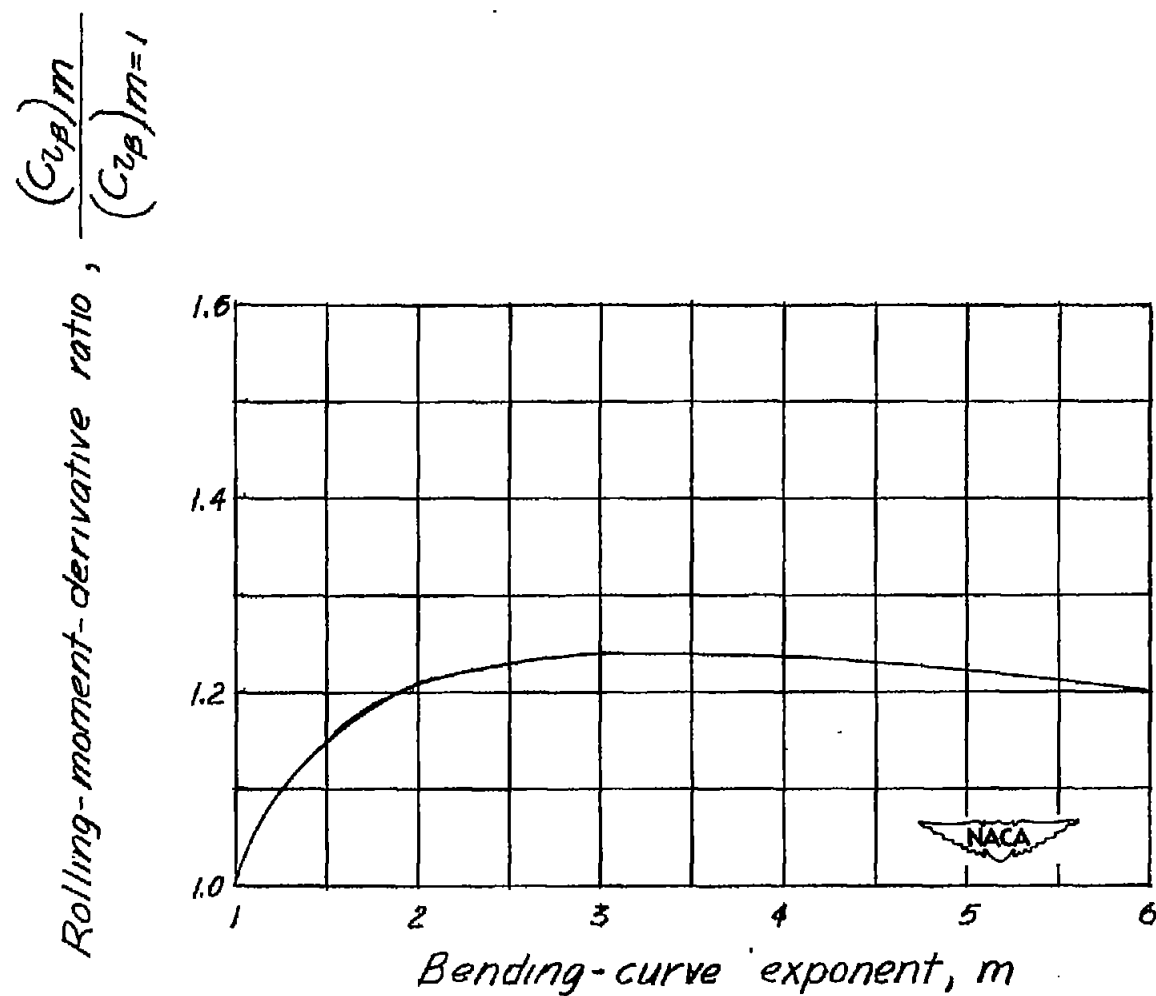


Figure 3.- Variation of bending-curve exponent with the rolling-moment-derivative ratio. $A=5$; $\lambda=0.50$.

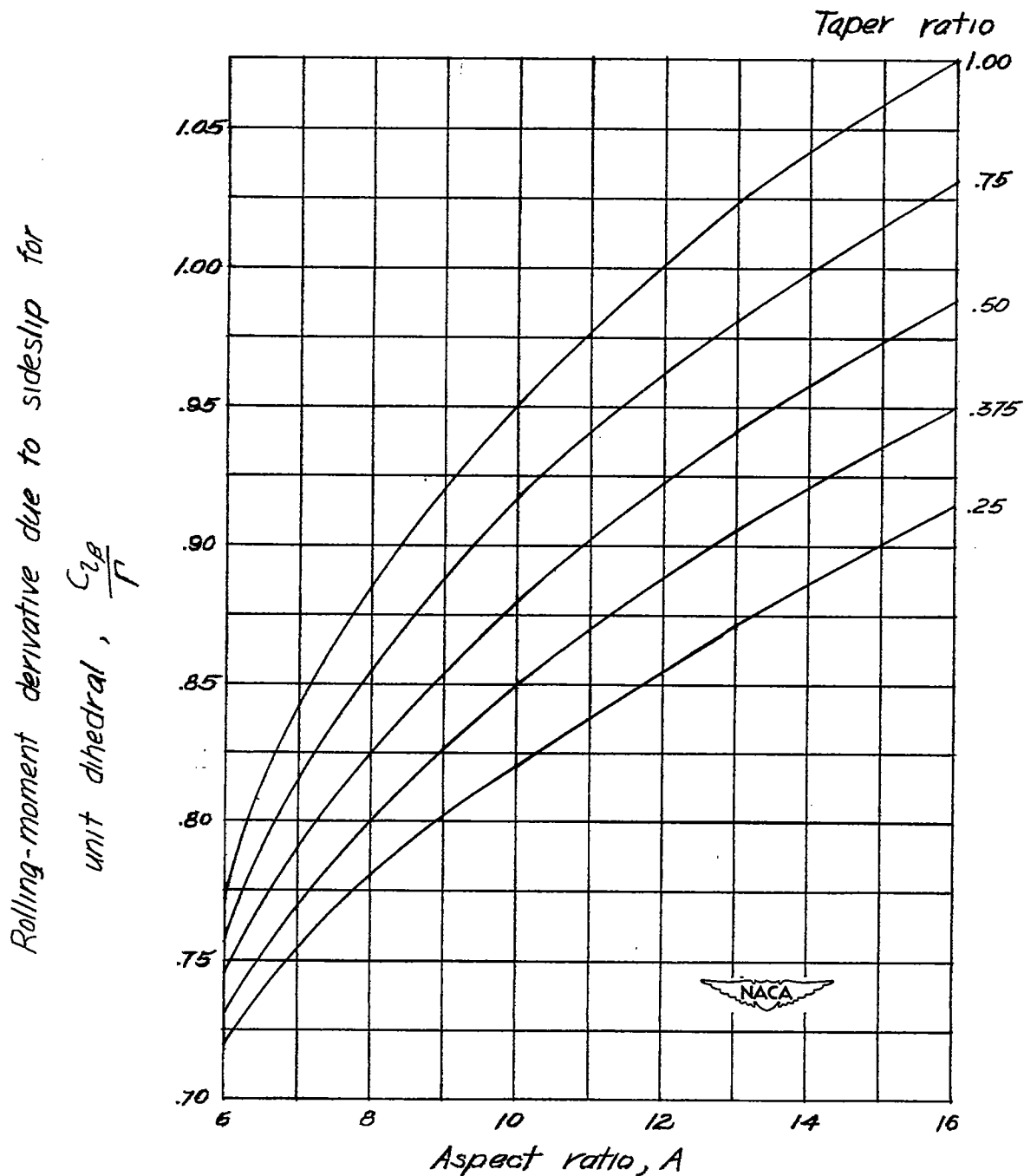


Figure 4.— Variation of rolling-moment derivative with aspect ratio and taper ratio for rigid wing ($m=1$).

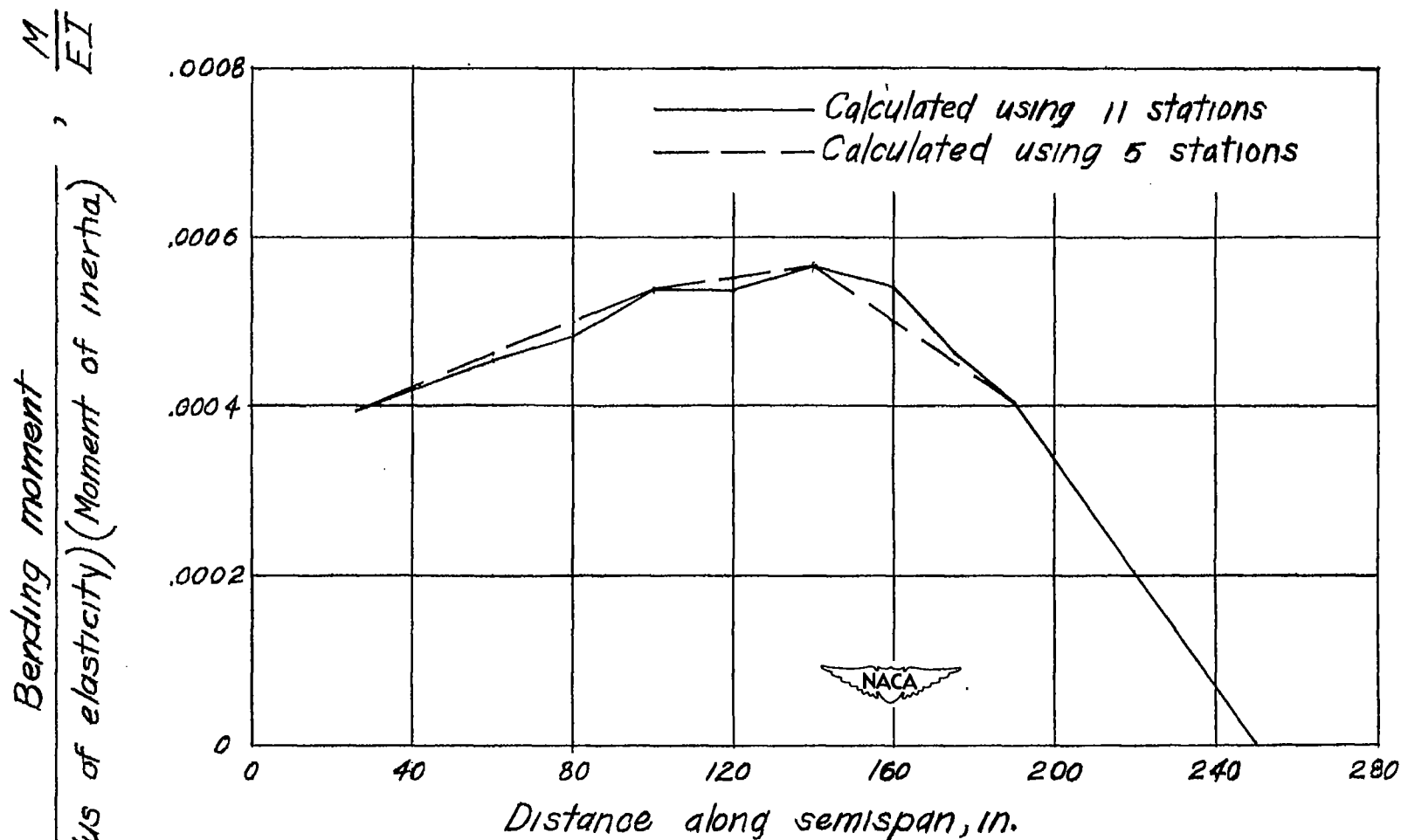


Figure 5.— The $\frac{M}{EI}$ -curve for a fighter-type airplane
at the limit load factor.

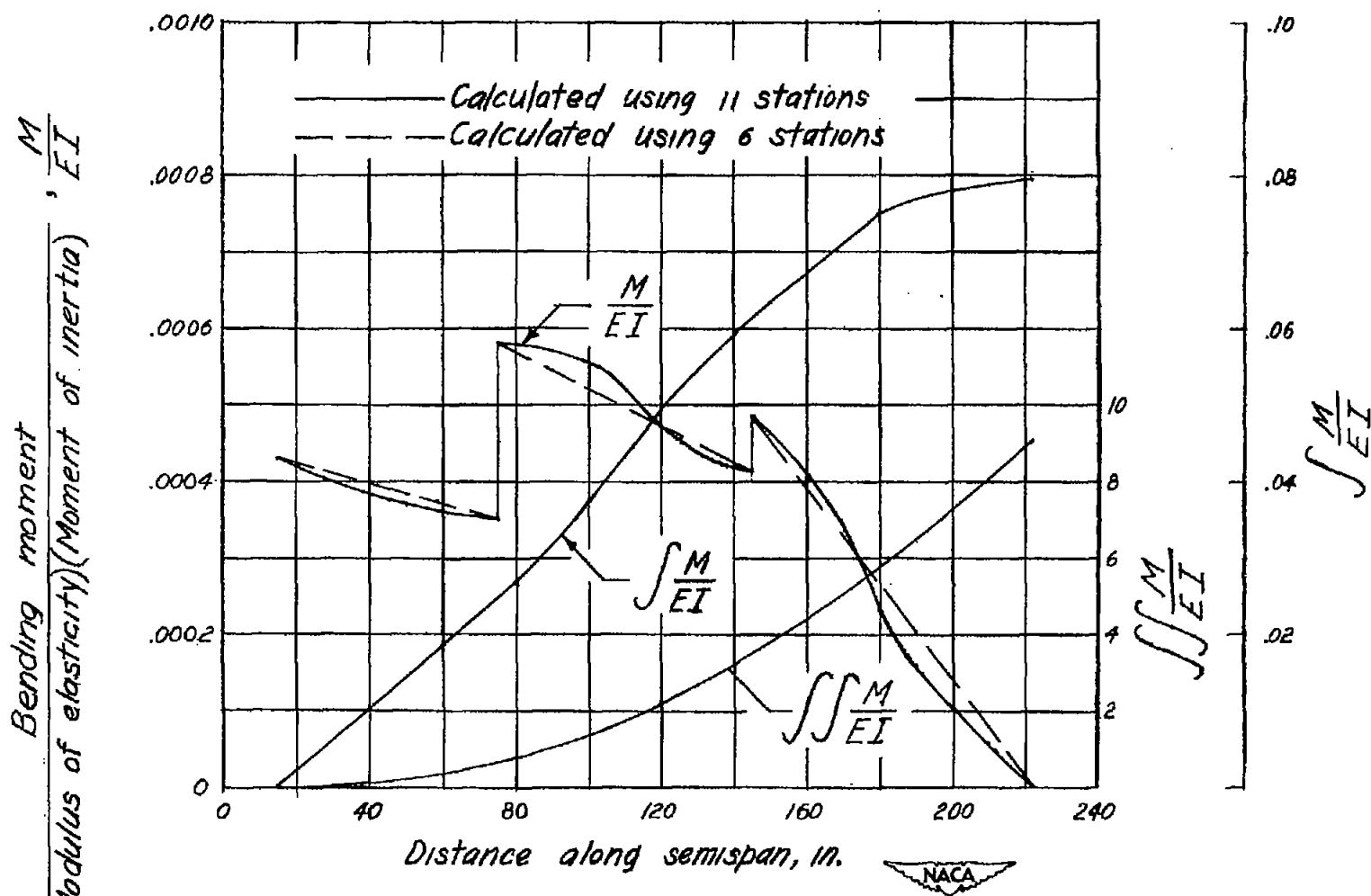


Figure 6.- The $\frac{M}{EI}$ -curve for a fighter-type airplane
at the limit load factor.

$\frac{M}{EI}$
 Bending moment
 (Modulus of elasticity)(Moment of inertia)

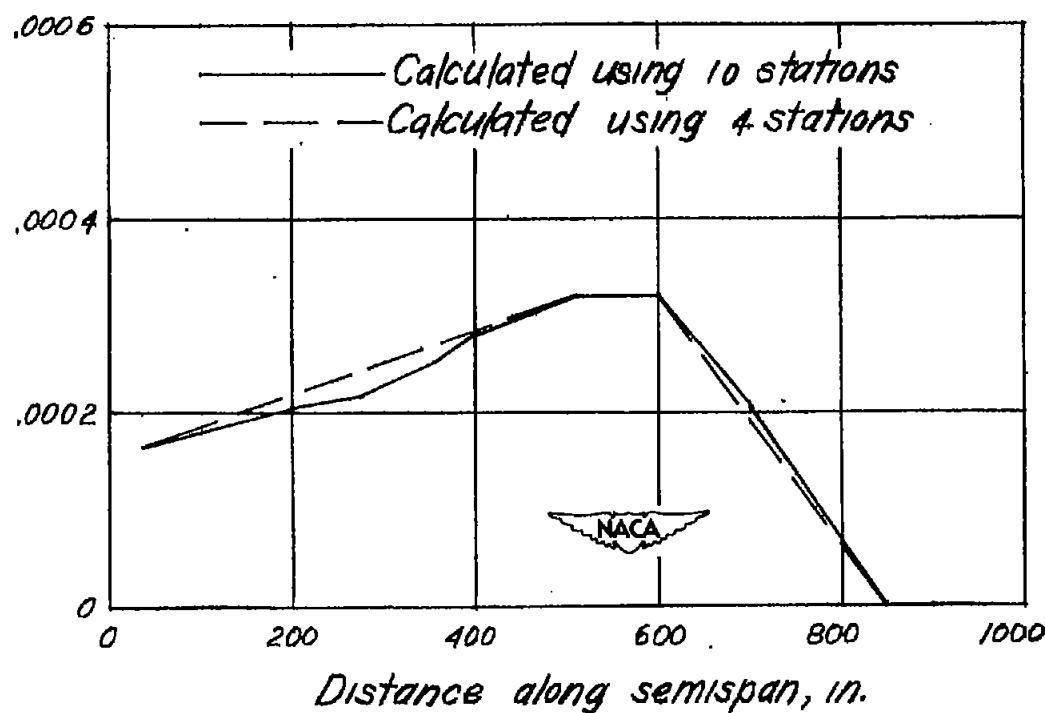


Figure 7.— The $\frac{M}{EI}$ -curve for a bomber-type airplane at the limit load factor.

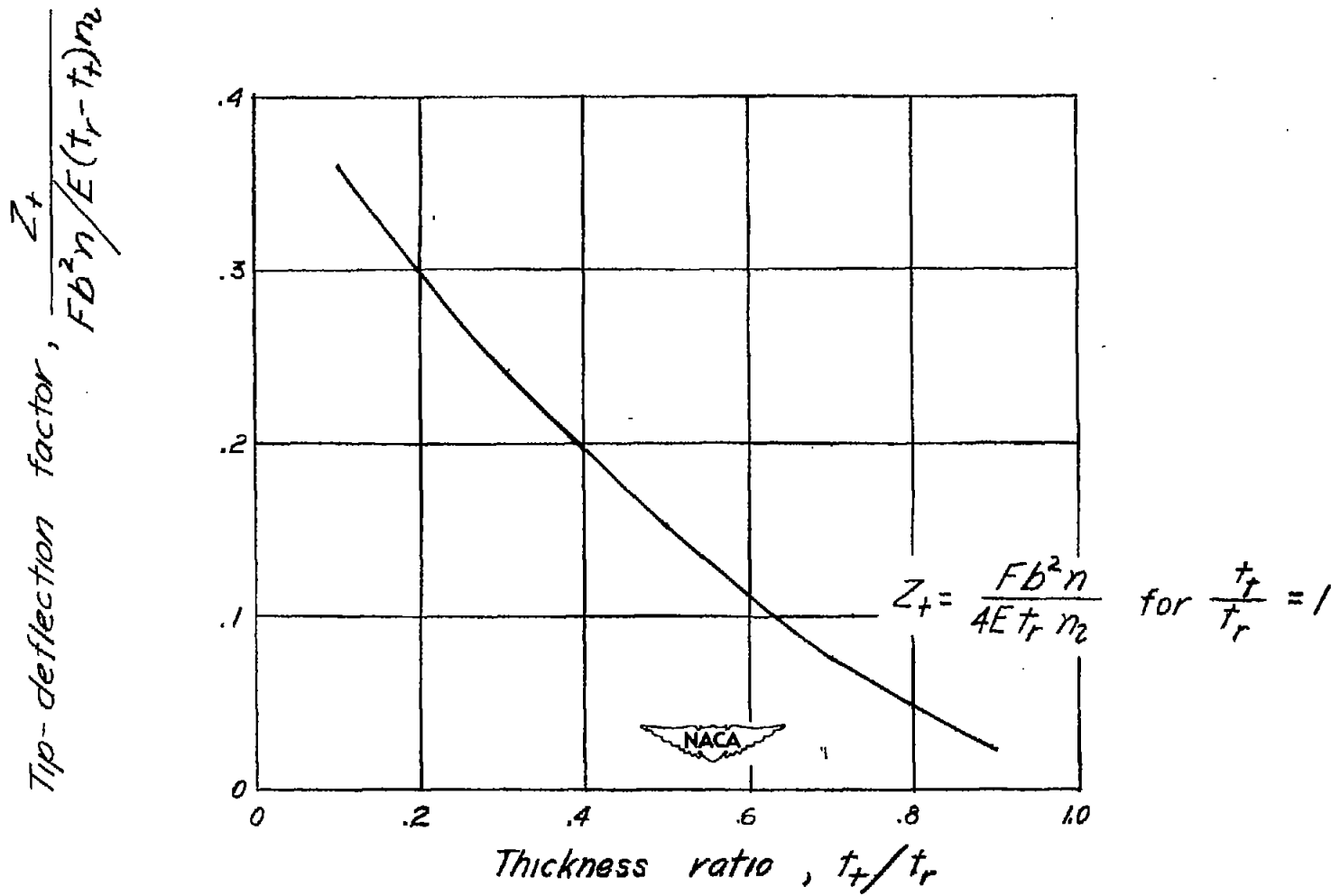


Figure 8.- Determination of tip-deflection factor.